CIRA 1972, RECENT ATMOSPHERIC MODELS, AND IMPROVEMENTS IN PROGRESS

L. G. Jacchia

Center for Astrophysics, Harvard College Observatory and Smithsonian Astrophysical Observatory, 60 Garden Street, Cambridge, Massachusetts 02138, USA

ABSTRACT

Work on the thermospheric section of CIRA 1972 was completed just before the first results from the new era of satellite-borne mass spectrometers could be utilized. The OGO 6 model (1974), although based on data collected within a limited range of height and solar activity (solar maximum), was a first step toward a new generation of models; similar in scope was the ESRO 4 model (1977), based on data recorded at lower heights and lower solar activity. The global Doppler-temperature model of Thuillier et al. (1977) provided a tool for discriminating between temperature and density variations and was utilized in the construction of the Jacchia 1977 model, which was based on a synthesis of temperature, mass-spectrometer, and total-density data from many sources. A similarly eclectic model is the MSIS model (1977), founded on incoherent-scatter temperatures and mass-spectrometer data from various sources. Each of the last two models has its strong and weak points, which are briefly discussed, together with suggestions for improvements. New models of the disturbed thermosphere by the author are compared with recent mass-spectrometer measurements at 170 km.

The first COSPAR International Reference Atmosphere (CIRA) was prepared by a committee chaired by Hilde Kallmann-Bijl and was submitted for approval and publication at the Second International Space Science Symposium in Florence, Italy, in April 1961. Three and a half years had elapsed from the launching of the first artificial satellite. During that meeting, the first man was launched into orbit, and Marcel Nicolet [1] presented a paper that immediately made the Reference Atmosphere obsolete: he showed that, above 100 to 120 km, the atmosphere was in diffusive equilibrium and that helium prevailed at the height of the Echo 1 satellite. Later that year, he produced a set of theoretical models based on these premises [2].

The CIRA committee became COSPAR Working Group 4, under the chairmanship of Wolfgang Priester. He lost no time in exploiting the new ideas, and by the following year, 1962, he presented to COSPAR the Harris-Priester model, which included dynamical features and became the core of the CIRA 1965 models above 120 km. In 1964, a set of empirical models was published [3], patterned after

Nicolet's theoretical 1961 models, and some of these formulae describing the different types of atmospheric variation also found their way into CIRA 1965.

COSPAR Working Group 4 expanded to encompass all the earth's atmosphere, neutral and ionized, equatorial and polar, and the CIRA committee continued within the framework of Panel 4A under the author's leadership. When the time seemed ripe, CIRA 1972 was published, in which the thermosphere and exosphere were modeled after a 1971 revision of the 1964 models [4]. As CIRA 1972 was being published, new factors were already at work that would make it obsolete. It was the publication, early in 1974, of the OGO 6 model [5], based on results from an orbiting mass spectrometer, that caused most of the obsolescence. Mass spectrometers had been orbited before, as early as 1962, but the perfunctory analyses of their measurements, spanning relatively short time intervals, had failed to reveal anything substantially new. The OGO 6 analysis, on the other hand, showed without any trace of doubt that there were new phenomena in the thermosphere that had to be taken into account. Temperature changes caused changes in composition as a result, not only of changes in the scale height of the individual constituents, but also of related convective phenomena.

The OGO 6 model had been derived from 2 years (1969 to 1971) of measurements in the height range from 400 to 600 km under quiet geomagnetic conditions. It assumed fixed boundary conditions at 120 km and derived its temperatures from N_2 variations. The variation with height of the density of three constituents (N_2, O, He) was computed from a Bates-Walker exponential approximation to the profiles, in which a single temperature-gradient parameter, s, was used throughout. The exospheric temperature was related linearly to the smoothed 10.7-cm solar flux $\bar{F}$ and quadratically to the instantaneous flux F. It was assumed that the types of atmospheric variation were those that had been more or less standardized in the Jacchia [3] models; each type of variation, however, was expressed as the sum of the smallest number of selected spherical harmonics deemed necessary to represent it adequately.

The all-important feature that made the OGO 6 model different from its predecessors was that the coefficients of these spherical harmonics were determined separately for each individual constituent. This meant that in the diurnal, annual, semiannual, and geomagnetic variation, each of the constituents was free to vary in its own individual way — and these ways turned out to be quite different. Of particular importance was the difference in behavior between N_2 and O because, in previous models, temperatures had been based mainly on total densities, which in the region covered by satellite drag is about equivalent to saying atomic oxygen densities. Temperatures determined from incoherent scatter had shown for some time substantial discrepancies in the phase of the diurnal variation and in the latitude of the temperature extrema at the solstices. Now, with the use of nitrogen temperatures, the discrepancies were minimized. If there had been any doubts about the soundness of the nitrogen temperatures, they were dispelled with the publication of the global temperature model by Thuillier et al. [6], which was based on Doppler temperatures derived from measurements of the 6300 Å airglow line by means of a Fabry-Perot interferometer on board the OGO 6 satellite. The temperatures were analyzed by using exactly the same spherical harmonics to represent the different types of atmospheric variations as in the OGO 6 model, and the results were very similar. An improvement over the latter model was the use of a linear relation between the temperature and the K_p index, instead of the a_p index, which permitted the analysis to be extended to geomagnetically disturbed days.

Measurements of N_2, O, Ar, and He were obtained in the range from 240 to 320 km by the gas analyzer on the ESRO 4 satellite from December 1972 to April 1974, during times of low solar activity. Again, after selecting only data from

geomagnetically quiet days, the data were analyzed along exactly the same lines as in the OGO 6 model and led to the ESRO 4 model [7]. The addition of argon to the list of constituents provided a valuable extension to the range of atomic or molecular masses. A global model of the disturbed thermosphere from ESRO 4 data was given by Jacchia et al. [8].

In March 1977, a new model was published [9] (J77), in an effort to combine the results of the OGO 6 and ESRO 4 mass-spectrometer data, the Doppler temperatures, and satellite-drag densities. This single-handed effort was to be overshadowed by the publication in June 1977 of the 13-author MSIS model [10, 11], which was based on mass-spectrometer data from four satellites (OGO 6, San Marco 3, Aeros A, and AE-C) and incoherent-scatter temperatures from four stations (Arecibo, Jicamarca, Millstone Hill, and St. Santin). The MSIS model was constructed on the same general lines as the OGO 6 model; spherical harmonics were used to represent the individual types of global variation. Boundary conditions were again taken at 120 km, but a notable improvement was their variation as a function of local time, including that of the parameter s. Through this device, the shape of the curve representing the diurnal variation could be made to vary with height, with the semidiurnal component predominating at heights below 140 km and gradually being overwhelmed by the diurnal component as greater heights were reached — in agreement with the San Marco 3 and AE-C observations (Fig. 1).

While the OGO 6 and ESRO 4 models were ad hoc models, constructed to represent the measurements from a single experiment, the MSIS model tries to fit a variety of experiments. It includes six atmospheric constituents (N_2, O, O_2, Ar, He, and H) and covers a relatively wide range of solar activity. It is, therefore, the only model that can be directly compared with the Jacchia [9] models: except for the geomagnetic effect, the MSIS model gives a completely independent representation of the same atmospheric variations. The overall agreement between the two models is quite good.

Concerning the geomagnetic effect, the MSIS authors used a nonlinear relation between the geomagnetic index and the temperature, whose form is "similar to one suggested by Newton et al. (1965) and equivalent to one used by Jacchia (1968)." The trouble here is that the formula used by Newton et al. [12], namely

$$\Delta \log \rho = a + b \log A_p \quad , \tag{1}$$

has a singularity at $A_p = 0$, whereas Jacchia's [13] formula, which originally appeared in Jacchia and Slowey [14] and was reported in several subsequent papers, including the 1971 models, does not. The latter formula is

$$\Delta T = c_1 a_p + c_2[1 - \exp(c_3 a_p)] \quad . \tag{2}$$

The formula used in the MSIS model is

$$\Delta T = a_1(A_p - 4) + a_2\{(A_p - 4) + [\exp(a_3(A_p - 4)) - 1]/a_3\} \quad . \tag{3}$$

It fits both equations (1) and (2) for $A_p > 4$; for $A_p < 4$, however, it sharply deviates from equation (2). It does not quite become singular at $A_p = 0$, but it almost does: at the poles, the temperature difference between $A_p = 0$ and $A_p = 4$ amounts to 201 K (Fig. 2). Now, A_p is the daily mean of the 3-hourly a_p's and hardly ever (probably never) goes to zero, so the use of a formula with a near-singularity at $A_p = 0$ cannot have appreciably affected the MSIS analysis, which obviously must have used daily means.

The MSIS formula, however, presents a great inconvenience when one tries to cleanse the different atmospheric variations of the all-pervading geomagnetic effect by reducing the temperatures and densities to the ideal condition $A_p = 0$.

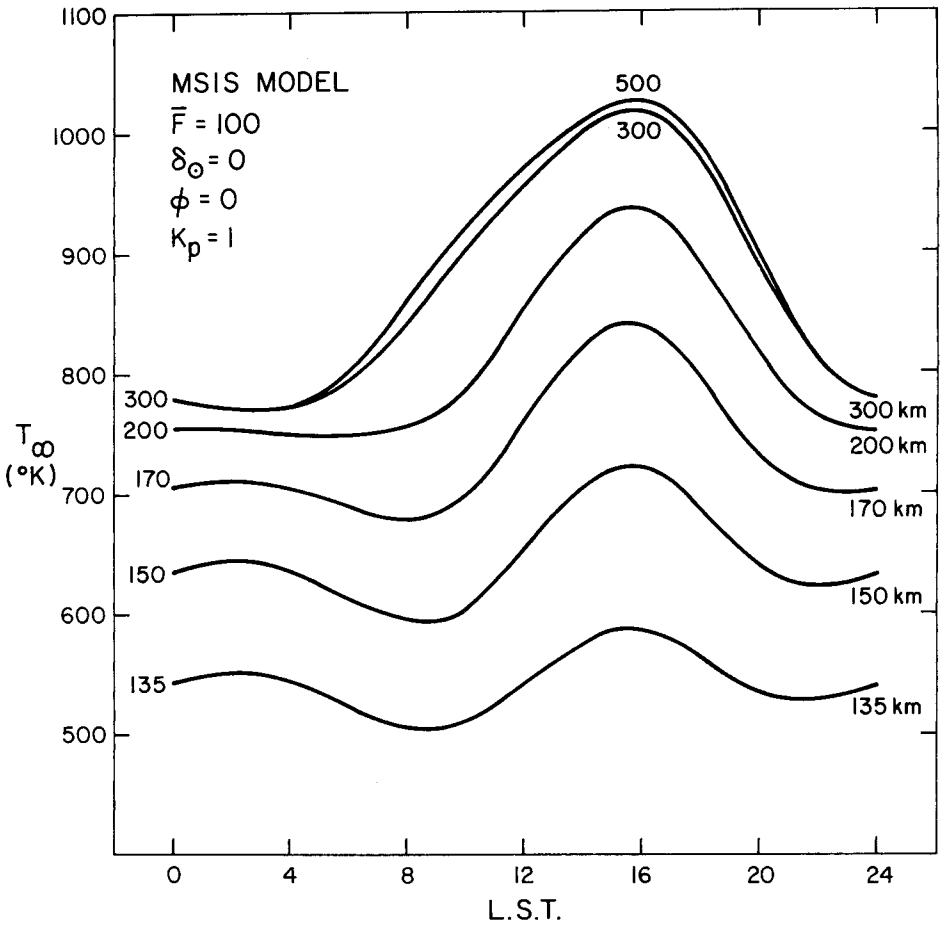

Fig. 1. Diurnal temperature variation at heights from 135 to 500 km according to the MSIS model [10]; $\delta_\odot$ is the declination of the sun, and ϕ is the geographic latitude.

The problem, of course, stems from the whimsical relation between K_p and a_p near the origins. The relation is usually referred to as being "quasi-logarithmic." The "quasi" comes from the forcing of K_p to be zero when a_p is zero. A correct relation between the two indices is one involving the sinh function. The equation

$$K_p = 1.89 \sinh^{-1} (0.154 a_p) \tag{4}$$

and its inverse

$$a_p = 6.5 \sinh (0.53 K_p) \tag{5}$$

give an excellent fit to the officially accepted tabulation of the two indices.

In the MSIS model, only the temperatures and densities at high latitudes are seriously affected by the near-singularity at $K_p = 0$. We should have no trouble, then, making our comparisons at the equator. Figure 3 shows the mean exospheric temperature at the equator at the time of the March equinox when $K_p = 0$, as a

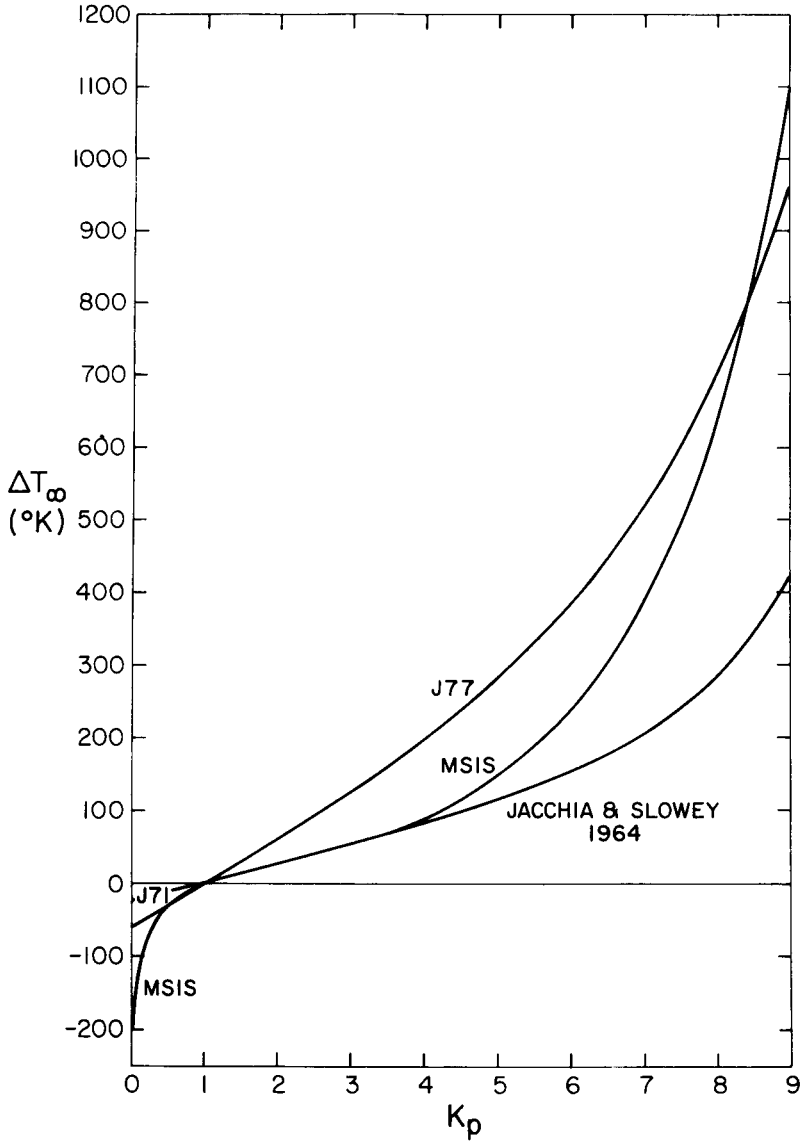

Fig. 2. The exospheric temperature (K) at the poles as a function of K_p in the MSIS model, compared with the corresponding relation in Jacchia and Slowey [14] and in the J77 model. In the latter model, the temperatures are those at the magnetic pole.

function of the smoothed 10.7-cm solar flux $\overline{F}$, under the condition $F = \overline{F}$, for the OGO 6, ESRO 4, MSIS, and J77 models, as well as for the temperature model of Thuillier et al. [6]. In the interval from $\overline{F} = 100$ to 250, the agreement between MSIS and J77 is nearly perfect; only for $\overline{F} < 100$ does J77 give lower temperatures. The difference arises essentially from the different shapes of the temperature profiles in the two models, which are more noticeable at low exospheric temperatures. A comparison of compositions in the four complete models (Fig. 4) also reveals substantial agreement. It must be emphasized that, in the J77 model, all

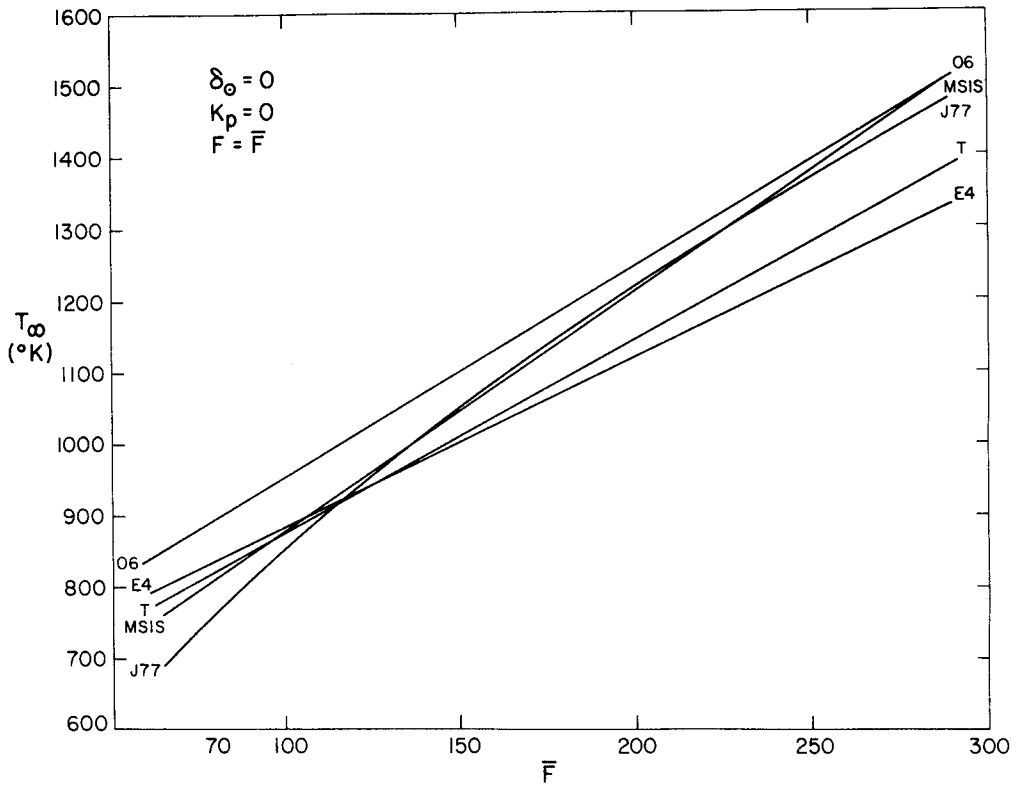

Fig. 3. Exospheric temperature as a function of the 10.7-cm solar flux F, when $F = \bar{F}$, according to five atmospheric models.

the number densities except those of O and O_2 are obtained directly from the sea-level composition by using a homopause height of 100 km, without any flux or empirical corrections. This includes argon and also helium, for which MSIS uses a correction. Argon and helium densities in J77 are in excellent agreement with the AE-C data at 150 to 200 km; at greater heights (450 to 1100 km), helium densities agree with OGO 6 and satellite-drag data.

Figure 5 shows the diurnal variation of the exospheric temperature at the equator for $K_p = 0$ at the time of the March equinox when $F = \bar{F} = 150$. The comparison of the five models shows the same systematic differences that can be seen in Fig. 3. It also shows a substantial agreement in the phases and the shapes of the curves; only the curve of the model of Thuillier et al. [6] shows a systematic shift to later hours.

Of considerable interest is a comparison of the temperature variations along a great circle through the poles with those through the points of maximum and minimum temperature (or as close as possible to the latter). When $K_p = 0$, the variation should be nearly sinusoidal, unless there is a permanent heat source of geomagnetic origin at high latitudes. In J77, no such extra source was assumed, but a distortion of the sinusoidal variation becomes noticeable even when K_p is as small as 0^+ or 1^-, owing to the strong latitudinal dependence of the geomagnetic effect (Fig. 6). Buckling at the poles in the curves reduced to $K_p = 0$ can be seen to some degree in the OGO 6, ESRO 4, and Thuillier et al. [6] models (Fig. 7). The MSIS model must be disqualified here because of its trouble

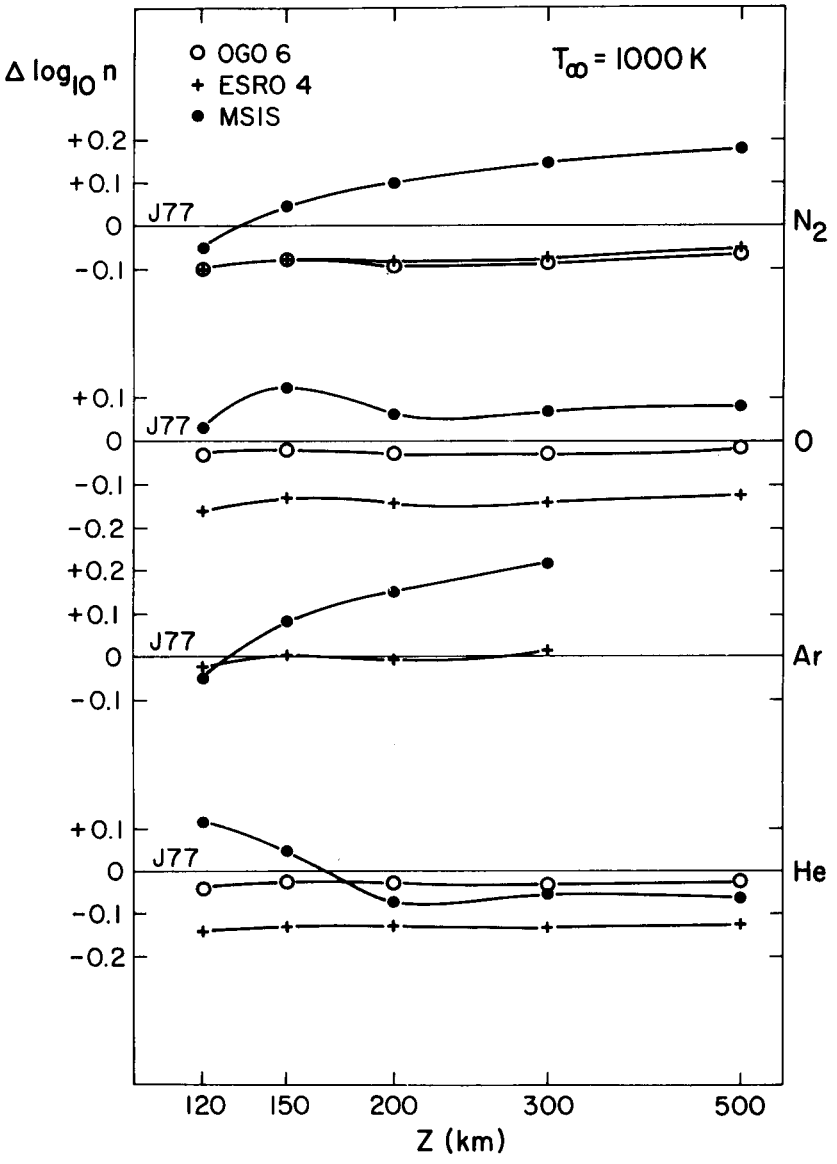

Fig. 4. Number densities of four species obtained from three models for an exospheric temperature of 1000 K, compared with those of the J77 model at different altitudes.

with the reduction to $K_p = 0$; the curve obtained for it actually shows a buckling in the opposite direction, as though there was a negative source of heat at the poles. As can be seen from Fig. 7, the humps are very different from one model to the next, and it is difficult to say whether there is any reality to them. We must remember that they can arise from two distinct causes: 1) an imperfect formulation of the geomagnetic effect, and 2) the inadequacy of the limited number of spherical harmonics to represent the temperature variation with latitude. Effects 1) and 2) are interacting, so it becomes very difficult to separate them,

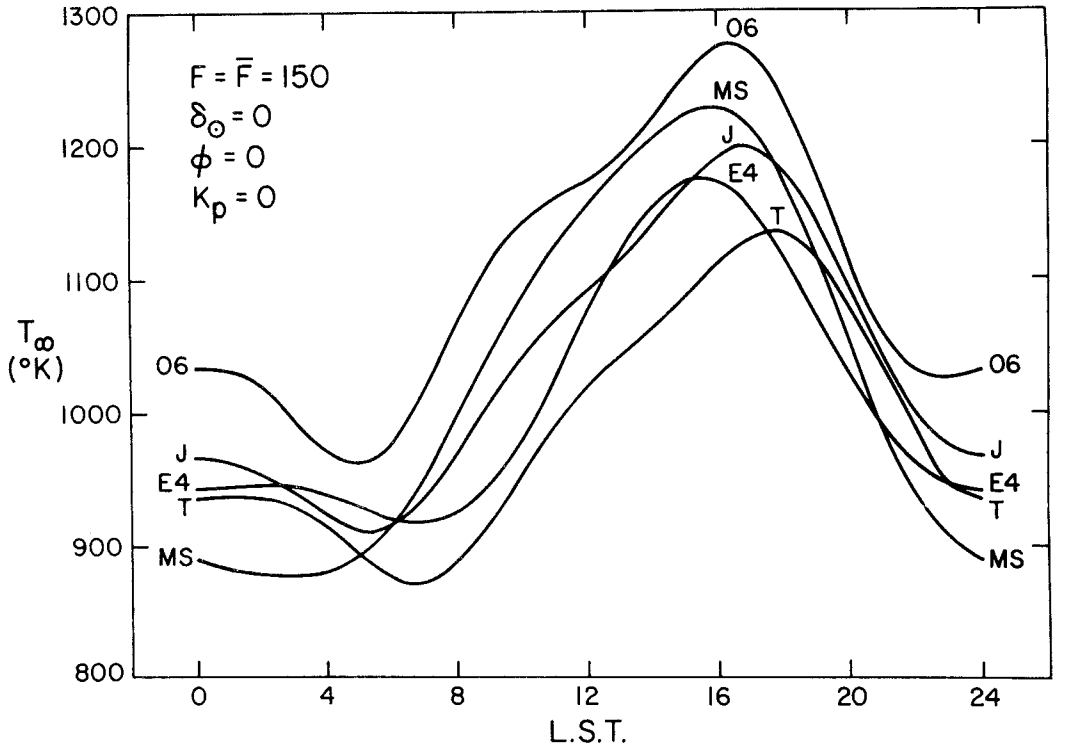

Fig. 5. Diurnal variation of the exospheric temperature at the equator at the time of the March equinox when $F = \bar{F} = 100$, according to five models.

and it is likely that harmonics determined in disturbed conditions will never vanish when $K_p = 0$, even if they should do so. In particular, attention is drawn to the double minimum stretching across the equator in the equinox curve. It is not present in Thuillier et al. [6], but it shows up in the OGO 6, ESRO 4, and MSIS models. But the double minimum in MSIS exhibits peculiar properties as $K_p = 1$ is changed to $K_p = 0$ (Fig. 8).

In any comprehensive analysis of atmospheric data, we first have to define the form of the equations that govern the variations and then determine by least squares the numerical coefficients in these equations. Where we have to deal with variations that depend on latitude and local time, it seems natural to use series of spherical harmonics: it is an objective procedure, in which no preconceptions are necessary; human judgment comes in only in deciding where to truncate the series or which terms to eliminate as being unnecessary. It is a very efficient method of analysis. The problem comes when we are faced with the results of several such analyses and want to make the best use of all this material, as we should for a future edition of CIRA. Comparing the coefficients of spherical harmonics is an impossibility unless the harmonics used are exactly the same (although in most cases they were). Besides, the harmonics are only an approximation to the true form of the variation, which may transpire from the results of the analysis and may be expressible in a more concise or physically more meaningful form. On the other hand, spherical harmonics afford a greater flexibility and uniformity and can more easily accommodate latitudinal asymmetries. It is important to point out some of the advantages and disadvantages of using spherical harmonics, in view of the popularity that they seem to be enjoying now.

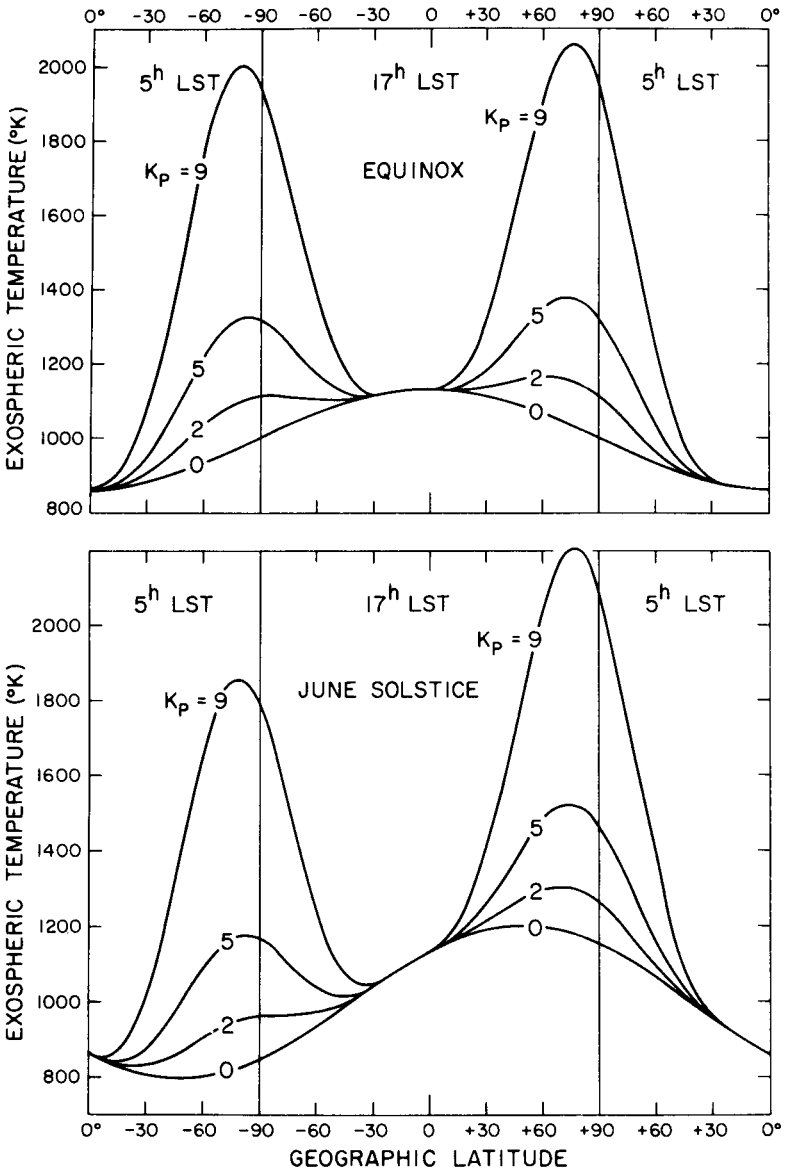

Fig. 6. Exospheric temperature profile along the complete (360°) meridional circle along which the local solar time is 17^h in one hemisphere and 5^h in the other, for various levels of geomagnetic activity, according to the J77 model, for a mean "quiet" temperature (K_p = 0) of 1000 K.

In the diurnal variation at heights below 200 km, MSIS has a distinct advantage over the J77 models, because it properly reflects the increased importance of the semidiurnal component. Because of the smallness of the diurnal variation at these low heights, the J77 models were not complicated to accommodate the deviations from the variations at greater heights that had been found in the San Marco data and confirmed by the ESRO 4 and AE-C measurements. According to

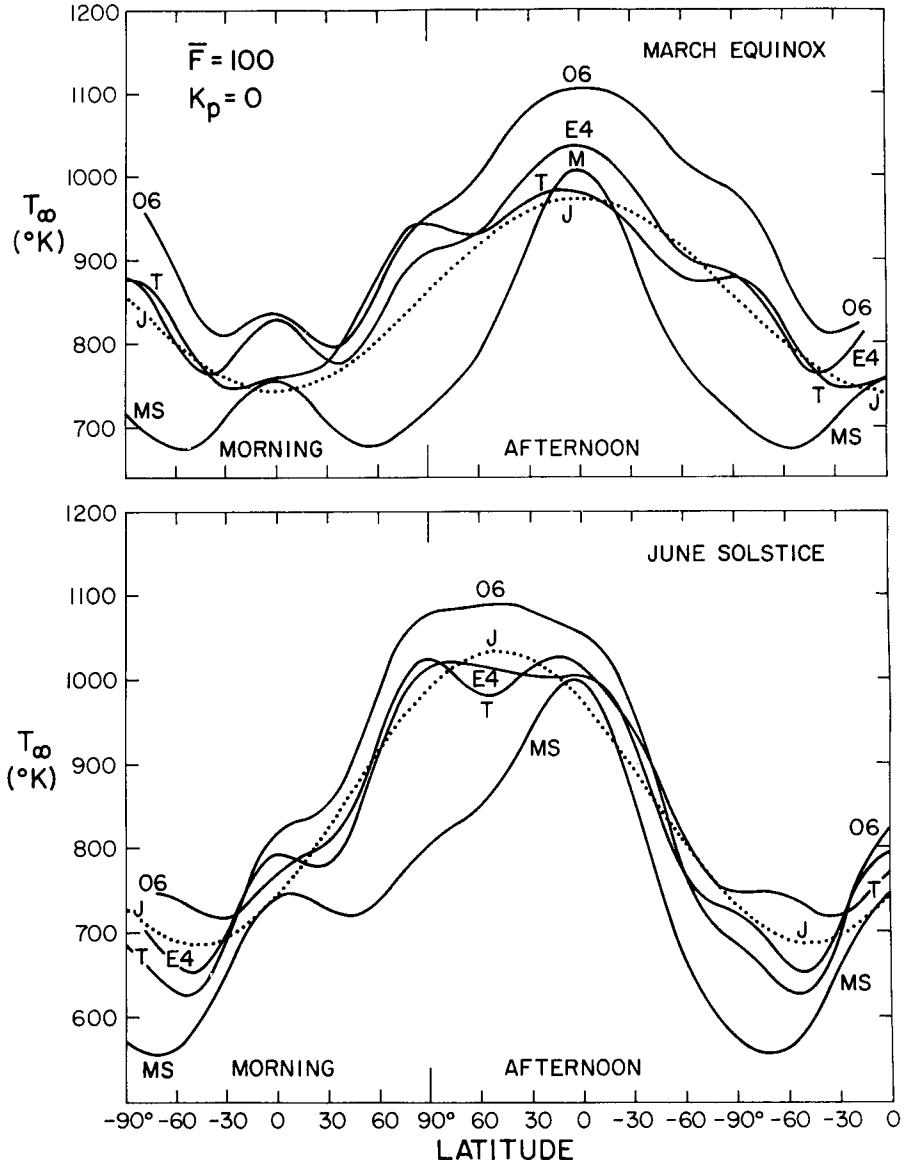

Fig. 7. Same as Fig. 6, but only for K_p = 0 and for $F = \bar{F}$ = 100, for five atmospheric models.

these data, only the phase of the helium variation below 300 km would require a correction in the MSIS model: the maximum density seems to occur about 1^h.5 earlier than the hour given by the model, 9^h.5 LST.

In the geomagnetic variation below 200 km, on the other hand, the situation is reversed: MSIS and all the other models fail to represent the observed amplitudes, while J77 is a good approximation to reality. Apart from making use of the invariant magnetic latitude, the model introduces a change in the shape of the

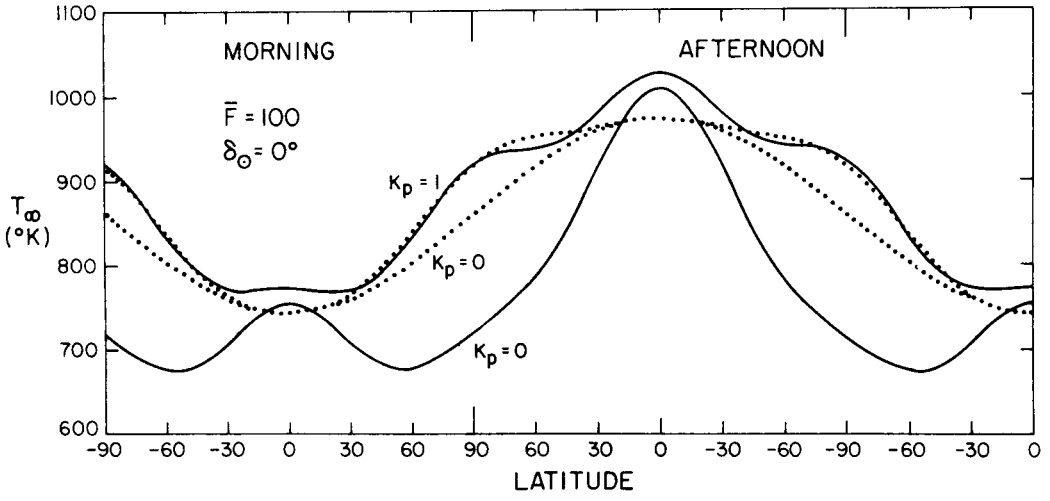

Fig. 8. Comparison of meridional profiles for K_p = 0 and K_p = 1, for the same conditions as in Fig. 7, in the MSIS (solid curves) and the J77 (dotted curves) models.

temperature profiles, which has the effect of greatly increasing the temperature in the 100- to 120-km region (Fig. 9), and thus of boosting the amplitudes of the density variations at low heights. Since the analytical expression that represents the temperature profiles is rather complex, it looked as though numerical integration would have to be used throughout, making use of the models prohibitively laborious. Fortunately, an analytical expression has been found that represents the results of the numerical integrations for any atmospheric constituent over the range of heights, "quiet" temperatures, and intensities of the geomagnetic perturbation currently covered by observations. As a result, the geomagnetic variation can be computed with no more trouble than, say, the diurnal variation. A comparison of the model with AE-C measurements of five atmospheric constituents at 170 km during a disturbed week in March 1974 is shown in Fig. 10. Work is in progress to improve both the form of the analytical expression and its coefficients to make its application as general as possible.

Acknowledgment. This work was supported in part by Grant NGR 09-015-002 from the National Aeronautics and Space Administration.

REFERENCES

1. M. Nicolet, J. Geophys. Res. 66, 2263 (1961).

2. M. Nicolet, Smithsonian Astrophys. Obs. Spec. Rep. No. 75, 1961.

3. L. G. Jacchia, Smithsonian Astrophys. Obs. Spec. Rep. No. 170, 1964; also in Smithsonian Contr. Astrophys. 8, 215 (1965).

4. L. G. Jacchia, Smithsonian Astrophys. Obs. Spec. Rep. No. 332, 1971.

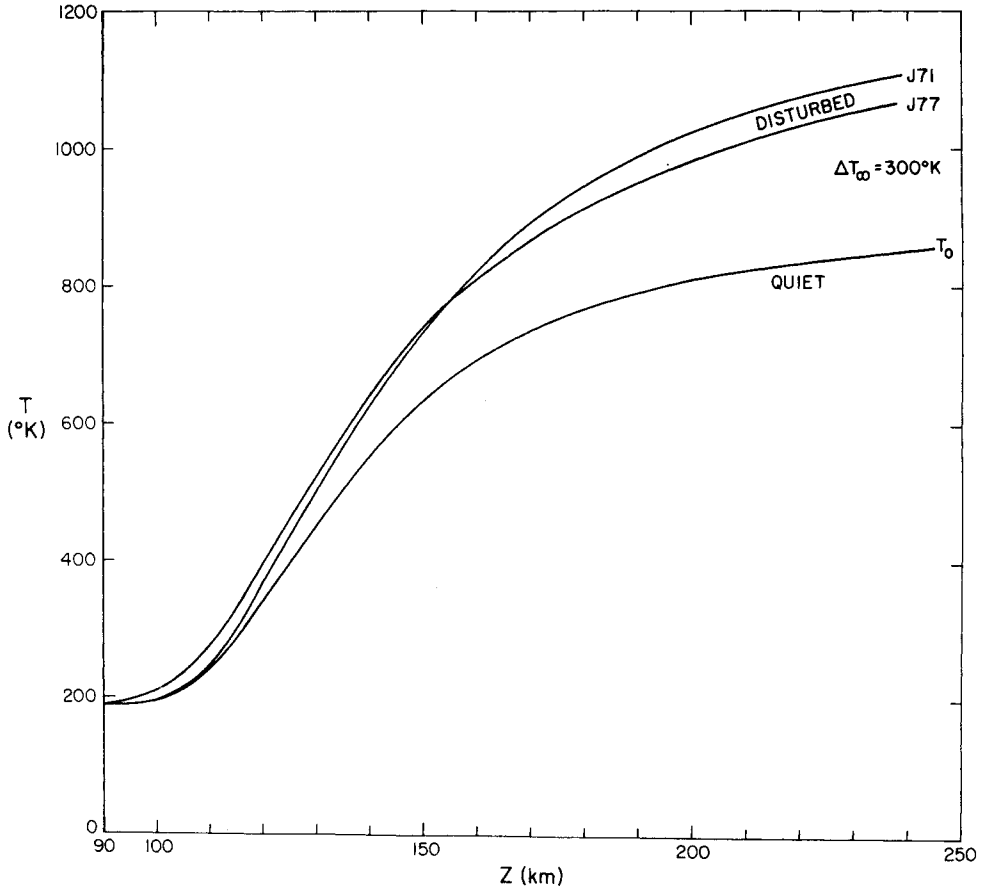

Fig. 9. A "quiet" (K_p = 0) and a "disturbed" (ΔT_∞ = 300 K) temperature profile according to the J77 model. The profile marked J71 is the profile that corresponds to the quiet exospheric temperature plus 300 K — i.e., the disturbed profile of the J71 model of the geomagnetic variation.

5. A. E. Hedin, H. G. Mayr, C. A. Reber, N. W. Spencer, and G. R. Carignan, J. Geophys. Res. 79, 215 (1974).

6. G. Thuillier, J. L. Falin, and C. Wachtel, Space Research XVII, 363 (1977).

7. U. von Zahn, W. Köhnlein, K. H. Fricke, U. Laux, H. Trinks, and H. Volland, Geophys. Res. Lett. 4, 33 (1977).

8. L. G. Jacchia, J. W. Slowey, and U. von Zahn, J. Geophys. Res. 82, 684 (1977).

9. L. G. Jacchia, Smithsonian Astrophys. Obs. Spec. Rep. No. 375, 1977.

10. A. E. Hedin, J. E. Salah, J. V. Evans, C. A. Reber, G. P. Newton, N. W. Spencer, D. C. Kayser, D. Alcaydé, P. Bauer, L. Cogger, and J. P. McClure, J. Geophys. Res. 82, 2139 (1977).

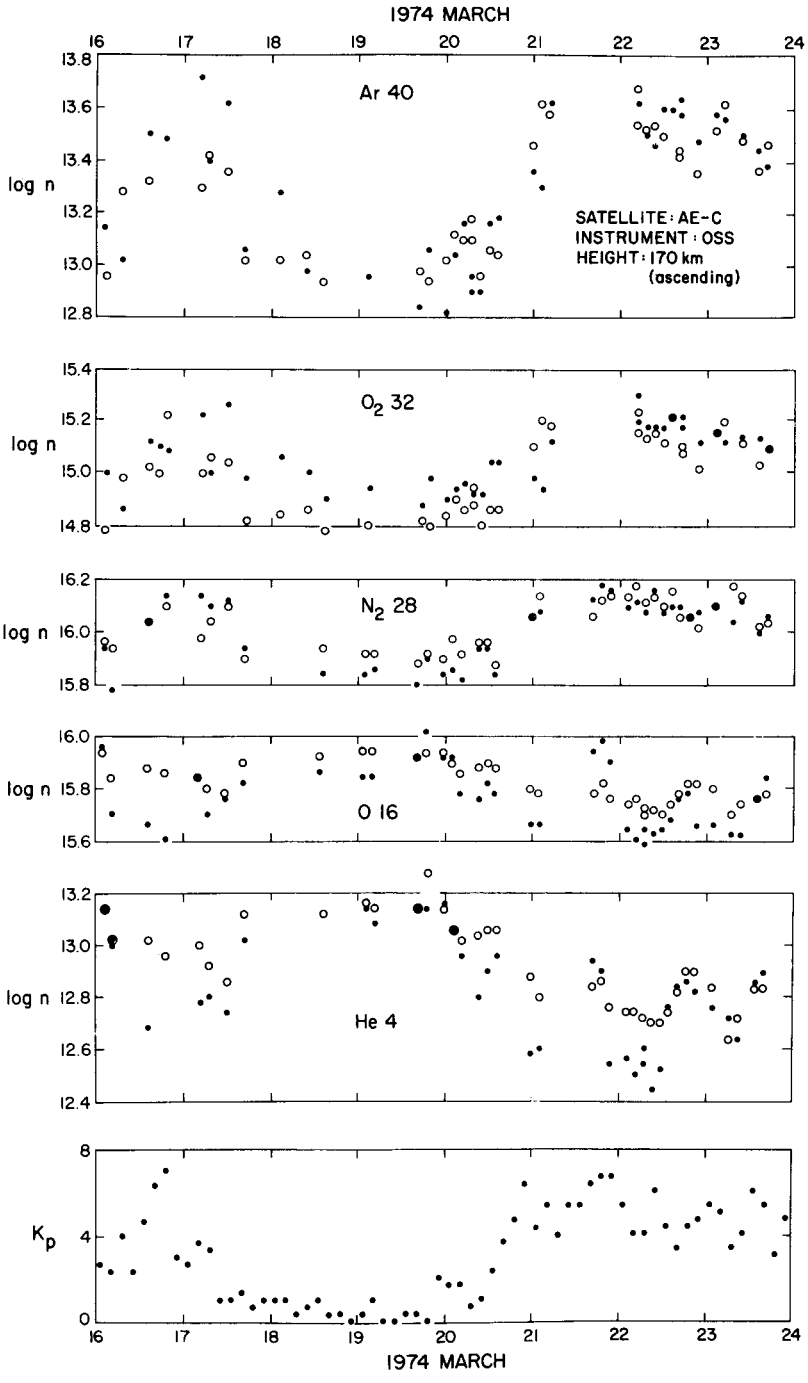

Fig. 10. Observed densities (per m^3) of five atmospheric constituents at 170 km from measurements on the OSS mass spectrometer on the AE-C satellite (dots) compared with densities computed from the J77 model (open circles).

11. A. E. Hedin, C. A. Reber, G. P. Newton, N. W. Spencer, H. C. Brinton, and H. G. Mayr, J. Geophys. Res. 82, 2148 (1977).

12. G. P. Newton, R. Horowitz, and W. Priester, Planet. Space Sci. 13, 599 (1965).

13. L. G. Jacchia, Space Research VIII, 800 (1968).

14. L. G. Jacchia and J. Slowey, J. Geophys. Res. 69, 4145 (1964).